9th Asia-Pacific Conference on Wind Engineering
Auckland, New Zealand
3-7 December 2017

POD analysis of wind field past rectangular buildings

F. Wang[1], K.M. Lam[2]

[1]Department of Civil Engineering
The University of Hong Kong, Pokfulam Road, Hong Kong

[2]Department of Civil and Environmental Engineering
The Hong Kong University of Science and Technology, Clear Water Bay, Hong Kong

Abstract

This paper investigates the characteristics of turbulent flow in the wake of two different building models. Particle image velocimetry is applied to measure the instantaneous velocity fields around the buildings. Proper orthogonal decomposition method is employed to analyze the complex turbulent flow field and the peak velocity excursions of each mode are extracted to reveal the dominant fluctuation patterns of the building wakes. The results suggest that these extreme patterns follow similar rules in influencing the instantaneous wind velocity fields while they are used to reconstruct the experimental data.

Introduction

Coherent structures which have been experimentally discovered were thought as important elements to understand the spatial and temporal characteristics of turbulent flows [6]. Based on the Karhunen-Loeve expansion, proper orthogonal decomposition (POD) was firstly applied by Lumley [7] to investigate these coherent structures. The main purpose of this method is to obtain a series of optimal linear modes with most of the energy of fluctuation for representing the original experimental or simulated data, making it possible to simplify the complicated fluid flow. Since then, this technique has gradually become a potentially useful statistical analysis tool in wind engineering (see e.g. [1,2,4]). The snapshot POD method proposed by Sirovich [8] is suitable to analyse velocity field data obtained experimentally from particle image velocimetry (PIV). Examples of PIV-POD studies in wind engineering include Kikitsu et al. [5] which decomposed the structures of wind velocity field in the wake region of a vibrating square-cross prism, and Kawai et al. [3] which reported the near wake structure behind a square prism with aspect ratio H/D = 2.7.

In the present study, time-resolved PIV measurements of wind velocity fields around different isolated building models are made in the wind tunnel. The snapshot POD method is applied to explore the coherent structures of the turbulent building wake velocity data. The extreme building wake patterns of lower-order modes are recognized and extracted. The ways of how they influence the instantaneous wind fields are discussed and summarized.

Experimental description

Wind Tunnel Test models

The experiments mentioned here were carried out in the boundary layer wind tunnel of the Department of Civil Engineering, The University of Hong Kong. The tunnel is of a recirculating type with a 12 m long working section of 3 m wide and 1.8 m tall. An inlet grid, triangular spires and floor roughness elements were used to generate a simulated atmospheric boundary layer at the centre of the turntable. The outlook of building models is shown in figure 1. The dimensions of the two models, in metres, are (height : width : depth) = (H : W : D) = (0.1 : 0.3 : 0.1) and (0.12 : 0.06 : 0.06). The mean wind speed profiles up to height H can be described by the power law with exponents at 0.16 and 0.25, respectively for the two models. The reference mean wind velocities in each case at the roof height of building models are approximately 5 m/s.

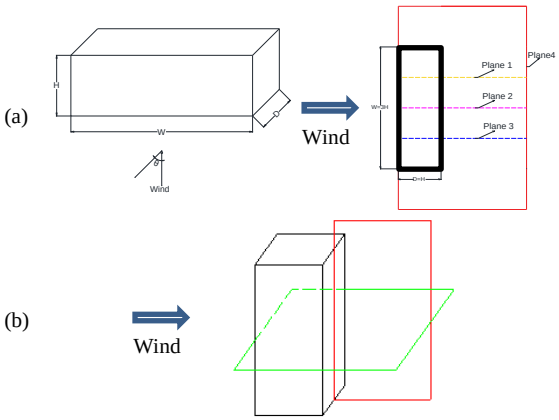

Figure 1. Test models and PIV measuring planes:
(a) Model 1; (b) Model 2

PIV Measurement

The turbulent wind fields around the building models were measured with time-resolved PIV. Air flow inside the wind tunnel was evenly seeded with dense mist with diameters at about 2-5 μm produced from 1:1 mixture of DEHS liquid and sunflower seed oil using a high volume liquid seeding generator. The measurement plane was illuminated by a thin laser sheet generated from the laser beam of a double-cavity Q-switched Nd:YAG laser. The double laser pulses were fired at 100 Hz, delivering an energy of 50 mJ per pulse with 0.2 ms time interval between the laser pulses. The double-framed flow images for model 1 were captured with a high-resolution CMOS camera of resolution 1920×1200 pixels. The framing speed was set at 100 Hz double-image to capture a time sequence of particle images of 1825-image length. A PIV camera with a lower resolution (640×480 pixels) was used for model 2. The framing speed was also set at 100Hz double-image to capture a time sequence of particle images of 4264-image length.

In model 1, turbulent velocity fields were obtained on four PIV measuring planes as shown in figure 1. Vertical plane 2 was aligned at the mid-width of the building and the other two vertical planes 1 and 3 were at ¼ width from the side walls. Horizontal plane 4 was at mid-height of the building. Similarly, for the model 2, the central longitudinal vertical plane was located behind the building model for observing the features of the building wake. The horizontal planes focused on wind flow on the sides and back area of the building. They were located at

heights, $z/H = \{1/3, 1/2, 2/3, 5/6\}$, and named L1, L2, L3 and L4 separately.

Results

Time-averaged wind velocity field

Figure 2 describes the mean flow streamlines on different vertical planes of the building models. In general, the structures of time-averaged wake flows are quite similar in that there is a large circulating bubble behind the building model in the time-averaged sense. Behind the bubble, the mean flow reattaches on the ground. Comparing the detailed results of figure 2(a)-(c) on model 1, we can find that the position of reattachment point is at about 2.5H behind the building on plane 2, and about 2.0H on planes 1 and 3. Moreover, the position of the vortex core of the recirculating bubble behind the model is at (x/H, z/H) ≈ (1.0, 1.0) on plane 2 which is obviously higher than those on plane 1 and 3.

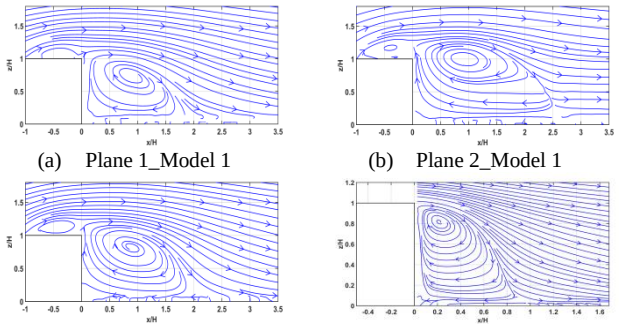

(a) Plane 1_Model 1 (b) Plane 2_Model 1

(c) Plane 3_Model 1 (d) Veritical Plane_Model 2

Figure 2. Mean flow streamlines of vertical planes

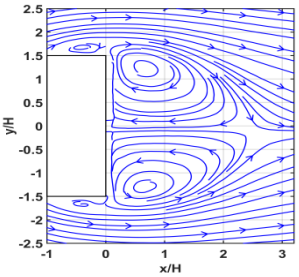

(a) Plane 4_Model 1

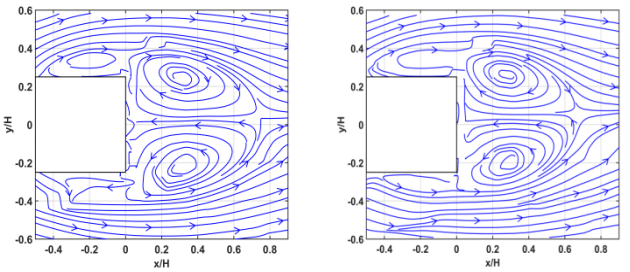

(b) L1 (1/3H) _Model 2 (c) L2 (1/2H) _Model 2

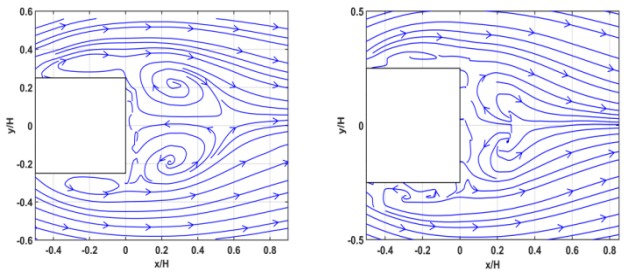

(d) L3 (2/3H) _Model 2 (e) L4 (5/6H) _Model 2

Figure 3. Mean flow streamlines of Horizontal Planes

Between the two buildings, observing the difference between figure 2(b) and 2(d), it can be found that the position of reattachment point of model 2 is markedly closer to the building. It is likely due to the different building width.

Figure 3 shows the mean flow streamlines on the different horizontal planes. As expected, the mean flow structures share a common axial-symmetry pattern. The wind flow separates at the side-walls and the separation streamlines join at a saddle point behind the building where the flow either returns upwind or escapes downwind. The results of model 2 show that positions of both the saddle point and the vortex core are different at different heights along the building, being closer to the building leeward wall at higher levels.

Energy distribution of POD modes

The wind field data acquired from PIV are analyzed using the snapshot POD method. Take the vertical plane 2 and horizontal plane 4 of model 1 as general examples. Figure 4 describes the cumulative energy of POD modes as well as the energy distribution of the first 20 modes. It is found that the energy of POD modes decreases dramatically with the mode number. The first two modes contain a large portion of the fluctuating energy, and they are used in the reconstruction process.

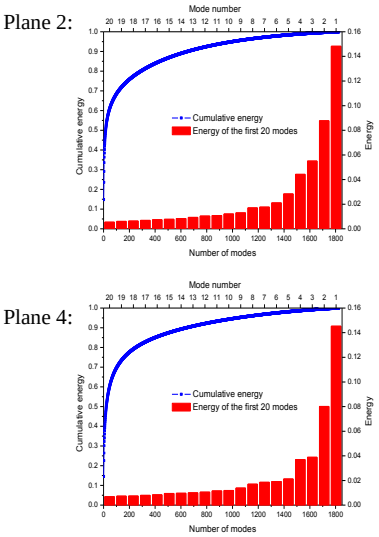

Figure 4. Cumulative energy of POD modes (left and bottom axes) and energy distribution of the first 20 modes (right and top axes), model 1

POD coefficients

The POD coefficients, $a_i(t)$, of the first 2 modes ($i = 1, 2$) are shown in figure 5. The coefficients vary with the time and in this study, the extreme values (maximum and minimum) are recognized and extracted, as marked in the figures. Here, t represents the time instant (or POD snapshot). When the POD modes are used to reconstruct the experimental data, the POD coefficients will directly affect the velocity fluctuations due to each mode. The extreme patterns at the peak time instants could exhibit the largest influence on the wind velocity fields due to the particular POD mode.

Extreme velocity patterns of POD modes

Figures 6-7 describe the streamlines of the extreme velocity fields on different vertical planes due to POD mode 1. They occur at the two peak instants of maximum and minimum $a_i(t)$. In addition to the mode 1 peak velocity fluctuations, the combined flow patterns with the time-averaged mean velocity field added are also shown to reveal the actual flow patterns at the extreme instants. It is obvious that the two extreme patterns

change the mean wind velocity field in two different extreme manners.

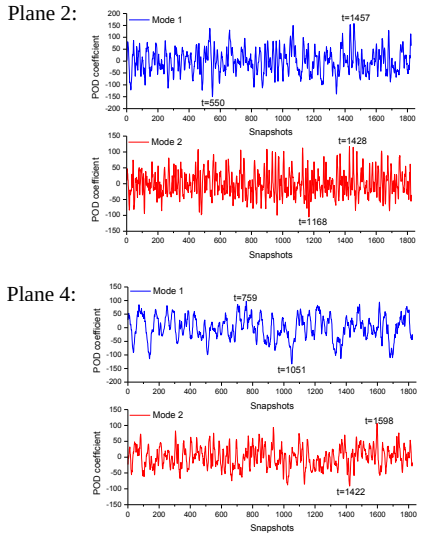

Figure 5. POD coefficients of first 2 modes, model 1

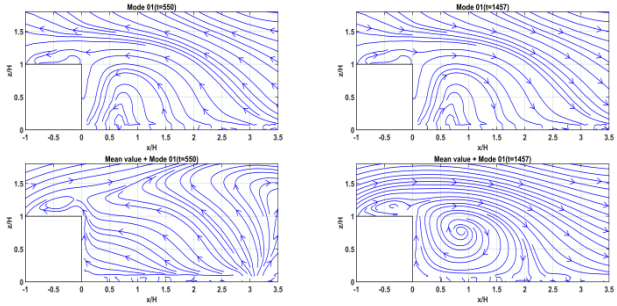

(a) extreme pattern at t = 550 (b) extreme pattern at t = 1457

Figure 6. Mode 1 extreme patterns on Plane 2 of Model 1
(First row: mode 1 velocity fluctuations; second row: with mean flow added.)

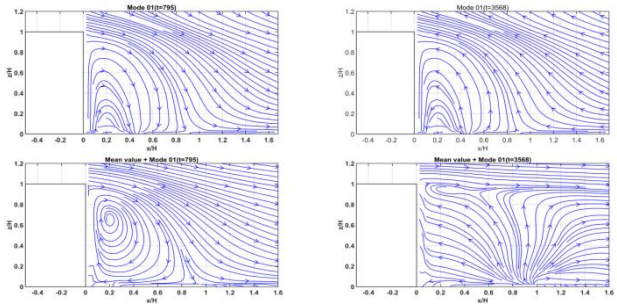

(a) Extreme pattern at t = 795 (b) Extreme pattern at t = 3568

Figure 7. Mode 1 extreme patterns on Vertical Plane of Model 2
(First row: mode 1 velocity fluctuations; second row: with mean flow added.)

Taking the vertical plane on model 2 (see figure 7) as an example, the positive extreme POD pattern, occurring at t = 795, has consistent directions as the mean velocities at almost all locations. It thus strengthens the characteristics of the mean flow. On the contrary, the negative extreme velocity fluctuations (at t = 3568) display totally opposite features. At the positive extreme, the peak mode 1 fluctuations often lead to a much strong recirculating vortex behind the building with much more intense and compact fluid circulation as compared to the mean flow in figure 2, with the position of vortex core much lower and closer to the building model. Conversely, when the negative extreme pattern occurs, the mode 1 fluctuations lead to disappearance of a well-organized vortex behind the building. The air flow is mostly upwind at almost the entire wake region. Similarly, for the other two vertical planes, the extreme velocity patterns of first POD mode show the same features. However, at both extreme instants, the turbulent kinetic energy of the velocity fluctuations, above the mean velocities kinetic energy, and due to mode 1, are the highest among all time instants. It should also be noted that although the two mode 1 peak velocity fluctuations are shown by the identical streamline patterns but of opposite flow directions, the magnitudes of the flow may be different.

For the influences of the two extreme patterns of mode 2, it seems to be more complicated. The streamlines of the extreme mode 2 velocity fields on some vertical planes are selected and shown in figures 8-9 for explanation and comparison. In the near-wake area, undoubtedly, the extreme patterns still play the same role as the mode 1, that is, positive for strengthening and negative for weakening. For instance, the circulating flow in the near wake of model 2 is greatly enhanced by the positive extreme pattern (at t = 2944, figure 9), with the reattaching point moving from 0.9H to 0.45H, showing a significant compression of the wind flow. On the contrary, the negative pattern (at t = 4181) results in a much longer reattaching point at 1.3H and a vortex core at (x/H, z/H) ≈ (0.7, 0.65). However, in the far-wake area, the extreme pattern influences the mean flow in a different way.

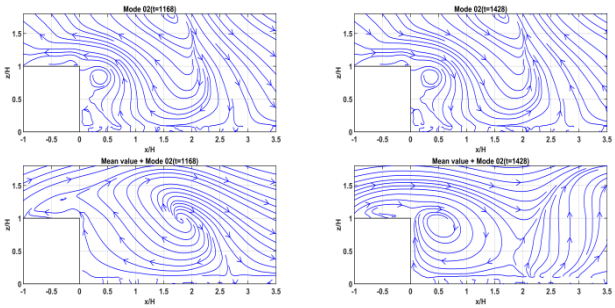

(a) extreme pattern at t = 1168 (b) extreme pattern at t = 1428

Figure 8. Mode 2 extreme patterns on Plane 2 of Model 1
(First row: mode 2 velocity fluctuations; second row: with mean flow added.)

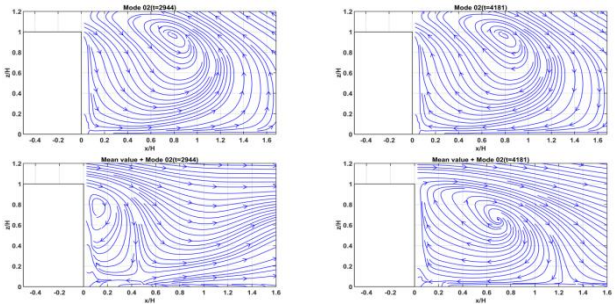

(a) Extreme pattern at t = 2944 (b) Extreme pattern at t = 4181

Figure 9. Mode 2 extreme pattern on Vertical Plane of Model 2
(First row: mode 2 velocity fluctuations; second row: with mean flow added.)

On the horizontal PIV planes, some interesting observations are obtained, and some results are shown in figures 10-11. Due to space limitation, only the first two modes on plane 4 of model 1 are shown here. And it is enough to describe the general features on the influence manners of the extreme patterns. The two extreme patterns of mode 1 destroy the symmetry of streamlines while the mode 2 extreme patterns can still keep this feature. The extreme patterns of mode 1 strengthen the left or right part of the mean flow and weaken the other part while the extreme patterns of mode 2 strengthen or weaken the whole plane at the same time.

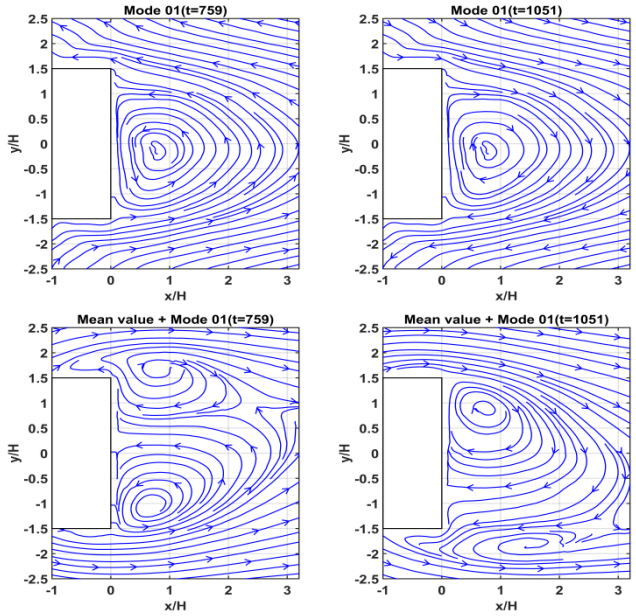

(a) extreme pattern at t = 759 (b) extreme pattern at t = 1051

Figure 10. Mode 1 extreme patterns on Plane 4
(First row: mode 1 velocity fluctuations; second row: with mean flow added.)

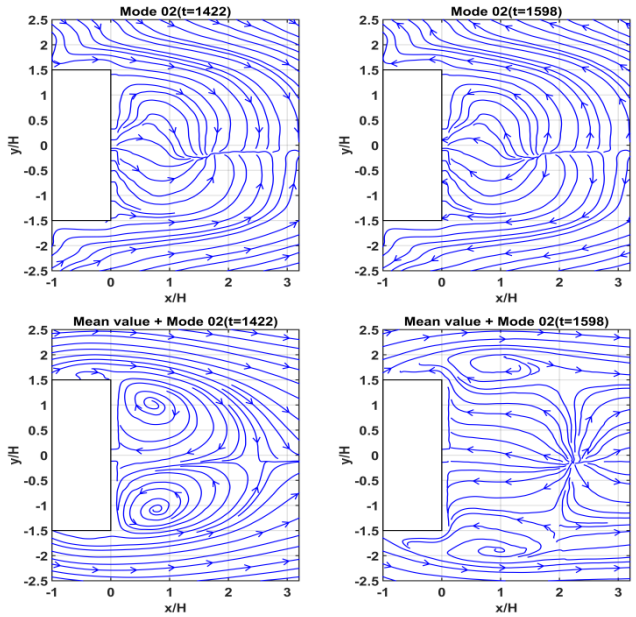

(a) extreme pattern at t = 1422 (b) extreme pattern at t = 1598

Figure 11. Mode 2 extreme patterns on Plane 4
(First row: mode 2 velocity fluctuations; second row: with mean flow added.)

Conclusions

In this study, experimental PIV data in the wake of two different building models were measured and then decomposed by the snapshot POD method. The first two modes containing the relatively largest energy are used to reconstruct the instantaneous wind velocity field of lower orders. However, due to the time-varying feature of POD coefficients, the contribution or influence manner of the POD modes cannot clearly be observed. Therefore, the concept of extreme patterns is adopted and they are recognized simply through selecting the time instants when the maximum or minimum value of POD coefficient occurs. Through comparing the patterns of flow fields around different building models, several conclusions are drawn.

1) On the vertical plane, the positive peak mode 1 extreme pattern of velocity fluctuation always flows in the same direction with the mean flow and strengthen it obviously, while the negative one will weaken it, sometimes even causing the disappearance of vortex circulation behind the building. The contribution of mode 2 extreme pattern is more complicated. The positive extreme pattern still plays the same role as the mode 1 does in the near wake while in the far wake its function seems to be opposite. Due to the inconsistence of the near-wake and far-wake flow circulation, there may be a new vortex observed in the upper area.

2) On the horizontal plane, the mode 1 extreme patterns destroy the symmetry of streamlines while the mode 2 extreme patterns can still keep this feature. The extreme patterns of mode 1 strengthen the left or right part of the mean flow and weaken the other part while the extreme patterns of mode 2 strengthen or weaken the whole plane at the same time.

Acknowledgments

The study is supported by a research grant awarded by the Research Grants Council of Hong Kong (HKU 713813E).

References

[1] Armitt, J., Eigenvector analysis of pressure fluctuations on the west instrumented cooling tower. *Internal Rep*, Central Electricity Research Laboratories, UK, 1968, RD/L/N114/68.

[2] Holmes, J.D., Sankaran, R., Kwok, K.S.C., & Syme, M.J., Eigenvector modes of fluctuating pressures on low-rise building models. *J. Wind Eng. Ind. Aerodyn.*, 69–71, 1997, 697–707.

[3] Kawai, H., Okuda, Y. & Ohashi, M., Near wake structure behind a 3-D square prism with the aspect ratio of 2.7 in a shallow boundary layer flow. *J. Wind Eng. Ind. Aerodyn.*, 104-106, 2012, 196-202

[4] Kho, S., Baker, C., & Hoxey, R., POD/ARMA reconstruction of the surface pressure field around a low rise structure. *J. Wind Eng. Ind. Aerodyn.*, 90, 2002, 1831-1842.

[5] Kikitsu, H., Okuda, Y., Ohashi, M., & Kanda, J., POD analysis of wind velocity field in the wake region behind vibrating three-dimensional square prism. *J. Wind Eng. Ind. Aerodyn.*, 96, 2008, 2093-2103.

[6] Liu, J.T.C., Contributions to the understanding of large scale coherent structures in developing free shear flows, *Advances in Applied Mech.*, 26, 1988, 183–309.

[7] Lumley, J.L., The structure of inhomogeneous turbulent flows. *In: Atmospheric Turbulence and Radio Wave Propagation* (eds. A.M. Yaglom, V.I. Tatarsky), Nauka, Moscow, 1967, 166-178.

[8] Sirovich, L., Turbulence and the dynamics of coherent structures. Part 1: Coherent structures, *Quart. Appl. Math.*, 45, 1987, 561-571.